

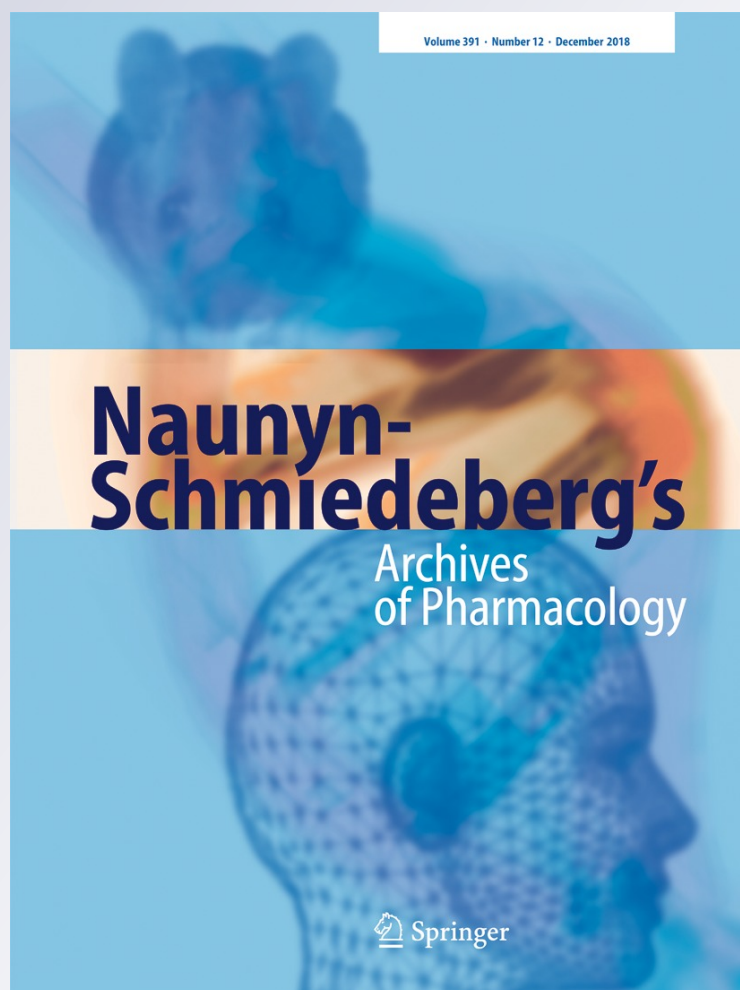
# *Antitumor activity of silver nanoparticles in Ehrlich carcinoma-bearing mice*

**Monira M. Rageh, Reem H. El-Gebaly &  
Marwa M. Afifi**

**Naunyn-Schmiedeberg's Archives of  
Pharmacology**

ISSN 0028-1298  
Volume 391  
Number 12

Naunyn-Schmiedeberg's Arch  
Pharmacol (2018) 391:1421-1430  
DOI 10.1007/s00210-018-1558-5



 Springer

**Your article is protected by copyright and all rights are held exclusively by Springer-Verlag GmbH Germany, part of Springer Nature. This e-offprint is for personal use only and shall not be self-archived in electronic repositories. If you wish to self-archive your article, please use the accepted manuscript version for posting on your own website. You may further deposit the accepted manuscript version in any repository, provided it is only made publicly available 12 months after official publication or later and provided acknowledgement is given to the original source of publication and a link is inserted to the published article on Springer's website. The link must be accompanied by the following text: "The final publication is available at [link.springer.com](http://link.springer.com)".**



# Antitumor activity of silver nanoparticles in Ehrlich carcinoma-bearing mice

Monira M. Rageh<sup>1</sup> · Reem H. El-Gebaly<sup>1</sup> · Marwa M. Afifi<sup>1</sup>

Received: 6 July 2018 / Accepted: 15 August 2018 / Published online: 3 September 2018  
© Springer-Verlag GmbH Germany, part of Springer Nature 2018

## Abstract

Silver nanoparticles (AgNPs) have a wide range of industrial and biomedical applications. The aim of the present study was to determine the cytotoxic and genotoxic effects of AgNPs on Ehrlich carcinoma-bearing mice. AgNPs were characterized by ultraviolet-visible absorption spectroscopy, dynamic light scattering, and transmission electron microscopy (TEM). Furthermore, the cytotoxicity and genotoxicity of AgNPs were evaluated using a series of assays: superoxide dismutase (SOD) enzyme activity, malondialdehyde (MDA) levels, DNA damage (comet assay), and histopathological examination of tissues and tumor size in Ehrlich carcinoma-bearing mice. Treatment of Ehrlich carcinoma-bearing mice with various concentrations of AgNPs (6, 24, and 48 mg/kg) injected intra peritoneal (IP) and intra tumor (IT) revealed that AgNPs significantly elevated the levels (0.5- to 5-fold) of MDA and reduced the activity (32–64%) of SOD. Furthermore, AgNPs caused a 2- to 3-fold increase in comet parameters such as percent tail DNA. Additionally, AgNPs inhibit the promotion of Ehrlich carcinoma by masses of necrotic and fragmented tumor cells. Consequently, the volume of tumor reduced by about 31–95% compared to control one. The results indicate that AgNPs possess cytotoxic and genotoxic effects against Ehrlich tumor and confirm the antitumor properties of AgNPs.

**Keywords** Ehrlich carcinoma · Silver nanoparticles · DNA damage

## Introduction

Cancer is considered as one of the most important causes of mortality in the world. Thus, there are many strategies available for cancer treatment. Currently, chemotherapy is still among the preferred strategy for clinical cancer treatment. However, chemotherapeutic agents used for treatment are expensive, induce serious side effects as well as drug resistance (Siegel et al. 2016; Bergfeld et al. 2014; Gottesman et al. 2002; Hill et al. 2008; Swain et al. 2003). Consequently, there was an urgent need to introduce a new approach to overcome these drawbacks.

Nanotechnology is a great scientific interest as it bridges the gap between bulk materials and atomic or molecular structures (Thakkar et al. 2010). Nanoscale particles display unique physiochemical properties which have enabled an improvement in its function and other properties. Nanotechnology has been expanding rapidly in recent years, impacting on diverse areas such as the economy and the environment, in addition to the increasing number of nanotechnology applications in medical diagnostics and therapeutics (Chen and Schluesener 2008). Recently, silver nanoparticles having fine or ultrafine sizes have attracted scientific attention due to its reliability, cost effective synthesis, and intrinsic properties. They are among the initial nanoproducts that have gained increasing interest in nanomedicine because of their cytotoxic, antimicrobial, anti-fungal, antioxidant, and anti-inflammatory effects (Kim et al. 2007; Kim et al. 2009; Kwon et al. 2012; Ebabe Elle et al. 2013). Additionally, they have been widely used in many applications, associated with environment and consumer products (Benn et al. 2010). The cytotoxic and genotoxic effect of AgNPs are dependent on their concentration, size, exposure time, surface-coating agents, and environmental factors (Narchin et al. 2018). Several Studies (Zapor Zapór 2016; Gliga et al. 2014; Park et al. 2011) indicate that silver

✉ Monira M. Rageh  
mrageh@sci.cu.edu.eg; monirarageh@yahoo.com

Reem H. El-Gebaly  
relgebaly@sci.cu.edu.eg; r\_elgebaly@msn.com

Marwa M. Afifi  
marwa.affi92@hotmail.com

<sup>1</sup> Biophysics Department, Faculty of Science, Cairo University, Giza, Egypt

nanoparticles, especially less than 10 nm, may be harmful to the organisms due to freely circulating within the body, and reach particular internal organs such as liver, spleen, kidneys, and lungs, consequently, interfere with cellular functions and cause toxic effects. The mechanism of their toxic effects is primarily mediated by increased production of free radical or reactive oxygen species (ROS). The overproduction of free radicals that leads to oxidative stress is caused by ions being released from silver nanoparticles. Consequently, genotoxicity seems to occur mainly via oxidative stress (Awasthi et al. 2013; Avalos et al. 2014). Additionally, Kalishwaralal et al. (2009) and Gurunathan et al. (2013a, 2013b) reported that AgNPs inhibit vascular endothelial growth factor (VEGF)-induced angiogenesis in bovine retinal endothelial cells. Several studies have reported the cytotoxic effects of AgNPs in different types of cancer and non-cancer cells, such as human alveolar epithelial cells, human breast cancer cells, and human ovarian cancer cells (Park et al. 2007; Han et al. 2014; Gurunathan et al. 2013a, 2013b; Yuan et al. 2017). In addition, Zielinska et al. (2018) concluded that AgNPs induced mixed type of programmed cell death in human pancreatic ductal adenocarcinoma and could provide a new therapeutic strategy to overcome chemo resistance in one of the deadliest human cancer. Prasannaraj et al. (2016) strongly suggested that the AgNPs showed potential anticancer activity of human liver and prostate cancer cell lines, hence, these studies showed antitumor, antiproliferative, and antiangiogenic effects of AgNPs in vitro. Moreover, Scoville et al. (2017) and Lin et al. (2017) conclude that silver nanoparticle-induced acute lung inflammation in mice and lethal bradyarrhythmias on myocardial electrophysiology. Also, Mata et al. (2018) and Wen et al. (2017) reported that the bio-distribution and extensive organ damages due to silver nanoparticles in vital organs of Wistar rats are arranged descending as follows: the liver, kidney, thymus, and spleen. Therefore, the liver was chosen in this work, because it is the most affected organ as revealed from previous studies. Because, there are limited studies on the toxicity of silver nanoparticles in carcinoma in vivo, it was very essential to study the synthesis and characterization of AgNPs first. Secondly, the cytotoxic and genotoxic effects of different doses of silver nanoparticles were investigated in the in vivo system using Ehrlich tumor bearing mice as a model and its side effects on liver were also studied. Thirdly, the probable mechanism of cell death caused by AgNPs was addressed with a series of assays, MDA level, SOD activity, and comet.

## Materials and methods

### Materials

Silver nitrate (MW 169.87), trisodium citrate (sodium citrate tribasic dehydrate MW 294.10), lipid peroxidation (MDA) kit,

and SOD determination kit were obtained from Sigma-Aldrich (Schnelldorf, Germany) and used without further purification.

### Preparation of silver nanoparticles

Silver nanoparticles were prepared by chemical reduction method according to the method of Turkevich et al. (1951). Briefly, silver nitrate (0.029 g) was dissolved in distilled water (100 ml), and the solution was stirred on a hot plate stirrer (MS-300HS, Misung Scientific, Gyeonggi-do, Korea) for boiling. 0.1 mol trisodium citrate was added drop by drop to the silver nitrate solution for reducing silver ions; the color gradually deepened.

### Characterization of silver nanoparticles

The absorption spectrum of AgNPs solution was measured by (JENWAY, 6405 UV/VIS. Spectrophotometer, Barloworld scientific, and Essex, UK) in the wavelength range 200–700 nm. The particle size, size distribution, and zeta potential for AgNPs were measured by the dynamic light scattering apparatus (Zeta potential/particle Sizer NICOMP-TM 380 ZLS, USA) at 25 °C dispersed in deionized water. The particle sizes and morphology of the AgNPs were examined using transmission electron microscopy (TEM) (FEI Tecnai G20, Super twin, Double tilt, LaB6 Gun) operating at 200 kV.

### Induction of mice with Ehrlich solid tumor and experimental design

Adult female BALB/c mice of average weight 25 g, 8–10 weeks of age were (obtained from National Cancer Institute “NCI,” Cairo University) injected subcutaneously with Ehrlich carcinoma cells (obtained from “NCI”) in their right flanks where the tumor was developed in a single and solid form as described by El-Bialy and Rageh (2013). All animal procedures and care were performed according to the guidelines for the Care and Use of Laboratory Animals, Cairo University Institutional Animal Care and Use Committee (CU-IACUC), based on reviewing the application number CU/I/S/12/16. Treatment Protocol was run on a total of 80 mice. Ten days after tumor cell inoculation, mice were randomly divided into two main groups. First group: animals ( $n = 40$ ) were divided into four sub-groups, (A): control group injected IP with PBS and groups (A1, A2, and A3) were injected IP with AgNPs with doses (6, 24, and 48) mg/kg respectively. Second group: animals ( $n = 40$ ) were divided into four sub-groups, (B): control group injected IT with PBS and groups (B1, B2, and B3) were injected with AgNPs with the same doses as the first group but the injection was IT. During the treatment protocol, the tumor volume was

monitored every 3 days over a period of 18 days for all the experimental groups and calculated according to Ning et al. (1994). At the end of the treatment, all the mice were sacrificed; tumor tissues and liver were quickly removed from each, rinsed with isotonic saline, divided into three parts, and used for evaluation.

### Oxidative stress analysis

The first part from tumor and liver tissues of mice from all groups' homogenates was prepared in cold phosphate-buffer. After their centrifugation (VS-18000M), the supernatants were used for estimation of SOD activity and MDA level. The SOD assay depends on the ability of the enzyme to prevent the phenazine methosulfate-mediated reduction of nitroblue tetrazolium dye measured at 560 nm (Nishikimi et al. 1972). Lipid peroxidation was measured by estimating the amount of malondialdehyde (MDA) according to Uchiyama and Mihara (1978). The colorimetric assay measures the reaction of MDA with thiobarbituric acid, giving a pink complex measured at 532 nm.

### Histopathology

The second part from tumor and liver tissues of mice from all groups was fixed in 10% neutral formalin, embedded in paraffin blocks, and sectioned and stained with hematoxylin and eosin (H&E). Tissue sections were observed under an optical microscope (CX31 Olympus microscope, Tokyo, Japan) connected to a digital camera (Canon).

### Comet assay (single cell gel electrophoresis)

Comet assay is considered as a rapid, simple, visual, and sensitive technique to evaluate DNA damage and early stage of apoptosis (Moller et al. 2000 and Awara et al. 1998). The comet assay was performed according to the method developed by Singh et al. (1988) and Tice et al. (2000). The third part from tumor and liver tissues of mice from all groups was used for the damage estimation of DNA by the method described by Rageh and El-Gebaly (2018). Comets were examined using a fluorescence microscope with magnification power  $\times 400$ . Comet 5 image analysis software developed by Kinetic Imaging, Ltd. (Liverpool, UK) linked to a CCD camera

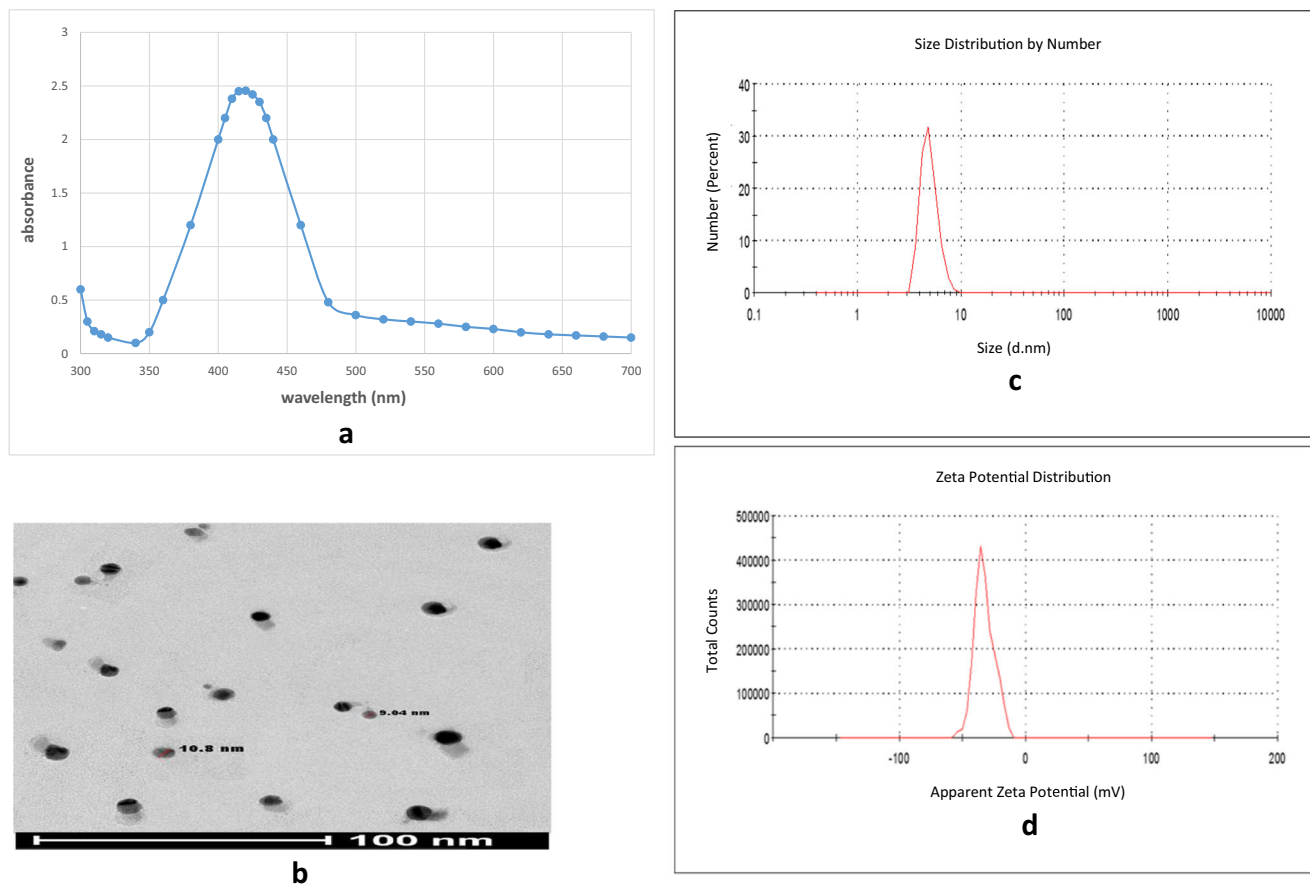


**Fig. 1** Characterization of AgNPs. **a** UV-visible spectrum. **b** Transmission electron microscope (TEM) image. **c** Size distribution. **d** Zeta potential of AgNPs

was used to measure DNA damage in 50 cells by measuring the length of DNA migration and the percentage of migrated DNA. Olive moment was computed (Moller 2006).

### Statistical analysis

The data were represented as the mean  $\pm$  standard deviation (SD) and were analyzed using SPSS v.19.0 for Windows. Significant differences between groups were assessed using one-way analysis of variance (one-way ANOVA); least-significant difference (LSD) was used for multi-groups comparisons.  $p < 0.05$  was considered significant.

### Result and discussion

Several studies have provided that generation of reactive oxygen species, in addition to the subsequent production of

oxidative stress play critical role in mechanisms of cytotoxicity genotoxicity induced by AgNPs. Abnormal accumulation of ROS will perturb the redox potential equilibrium, and finally result in a serious of cellular damages such as mitochondrial and DNA damage and finally cell death by apoptosis or necrosis (Foldbjerg et al. 2009; Piao et al. 2011; Kim and Ryu 2013; Guo et al. 2013). Moreover, cytotoxicity and genotoxicity of AgNPs are strongly dependent on the size and dose (Carlson et al. 2008; Tiwari et al. 2011; Swanner et al. 2015).

In the current study, AgNPs were characterized using several techniques. UV-visible spectrum was used to confirm the formation of silver nanoparticles. Figure 1a shows the absorption spectrum of AgNPs which have a strong and single surface plasmon resonant band at 360–480 nm, a maximum absorption peak at 420 nm (Pacioni et al. 2015 and Zhou and Wang 2012). The morphology and size of AgNPs were examined by TEM Fig. 1b. TEM image shows a well-dispersed and

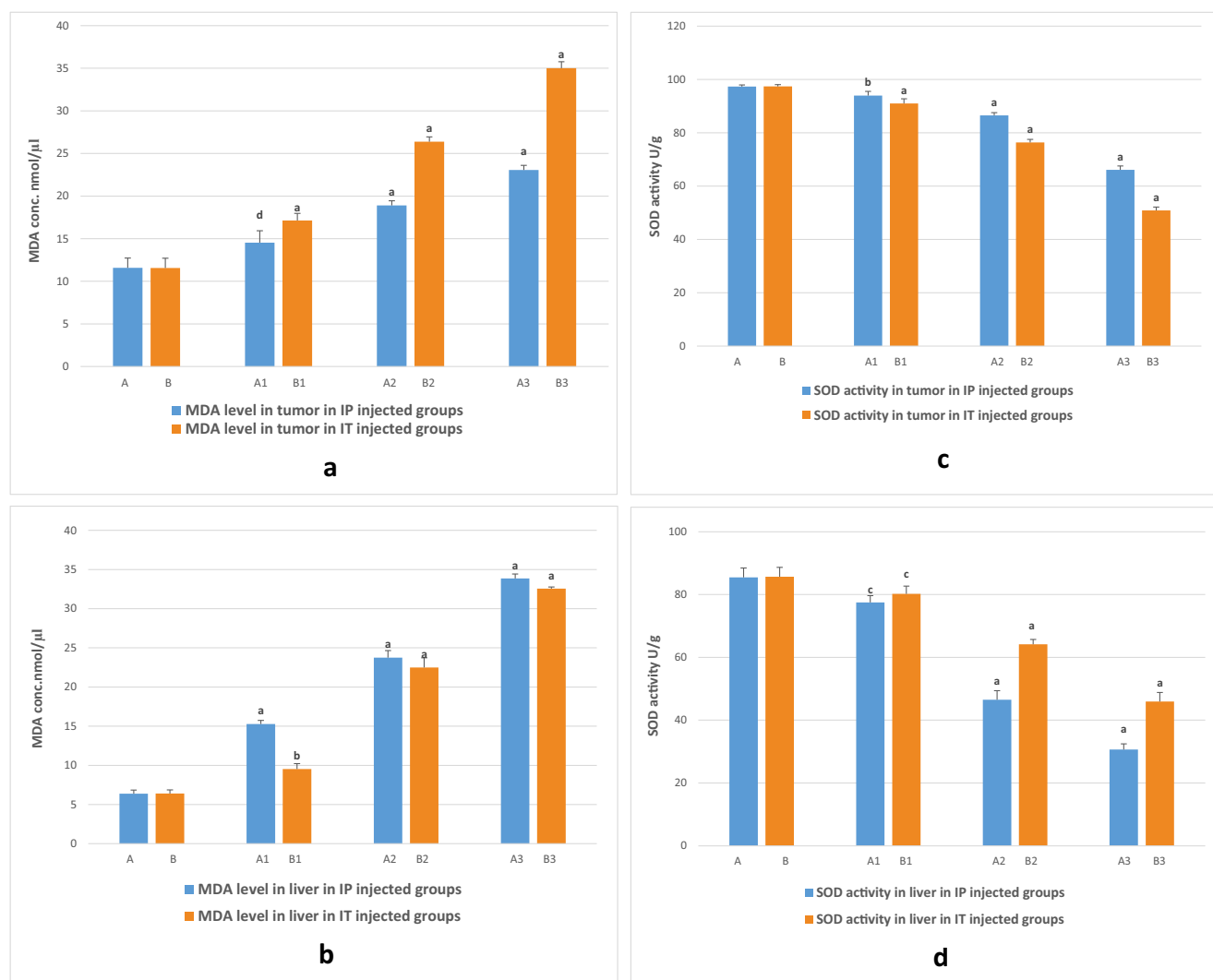


**Fig. 2** Effect of different doses of AgNPs (6, 24, and 48 mg/kg) injected IP and IT on MDA level and SOD activity: **a, c** in tumor and **b, d** in liver tissues. The data points are represented as mean  $\pm$  SD ( $n = 3$ ). (a,  $p \leq 0.0001$ ; b,  $p \leq 0.001$ ; c,  $p \leq 0.002$ ; d,  $p \leq 0.006$ ; e,  $p \leq 0.01$ ) compared to the control group

not aggregated round-shaped nanoparticles that have a diameter of about  $9.8 \pm 0.8$  nm. This result is confirmed by dynamic light scattering (DLS) measurement as presented in Fig. 1c. The figure represents a typical size distribution graph for AgNPs. As shown in the figure, the size of AgNP is concentrated on 6 nm with relatively narrow distribution. The potential analyzer was used to determine the electro-kinetic surface potential for AgNPs (Fig. 1d). The values of zeta potential for AgNPs is  $-32.7 \pm 2.2$  mV. These results indicated that citrate-coated silver ions increased the surface negativity, resulted in a high stability and prevented the aggregation of the dispersed particles (Ratyakshi and Chauhan Ratyakshi 2009).

The cytotoxic and genotoxic potential of AgNPs on the solid Ehrlich carcinoma-bearing mice were evaluated by measuring the following parameters: tumor size, oxidative stress, histopathology of tumor, and comet assay

for cellular DNA of tumor for the mice were treated with AgNPs IP and IT at the end of treatment protocol. All these parameters were evaluated in the liver too, because the liver is one of the first tissues to suffer damage when the organisms are treated with foreign substances (El Mahdy et al. 2014). The effects of treatment with AgNPs on lipid peroxidation were measured as MDA, in tumor and liver tissues and are shown in Fig. 2a, b. Mice groups treated with AgNPs (administered either IP or IT) showed elevation of MDA levels in tumor tissues by approximately 2- and 3-fold respectively compared to control groups (Fig. 2a). Also, Fig. 2b shows an increase in the level of MDA in liver tissues in all groups treated with AgNPs and administered either IP or IT by approximately 6- and 5-fold respectively compared to control groups.

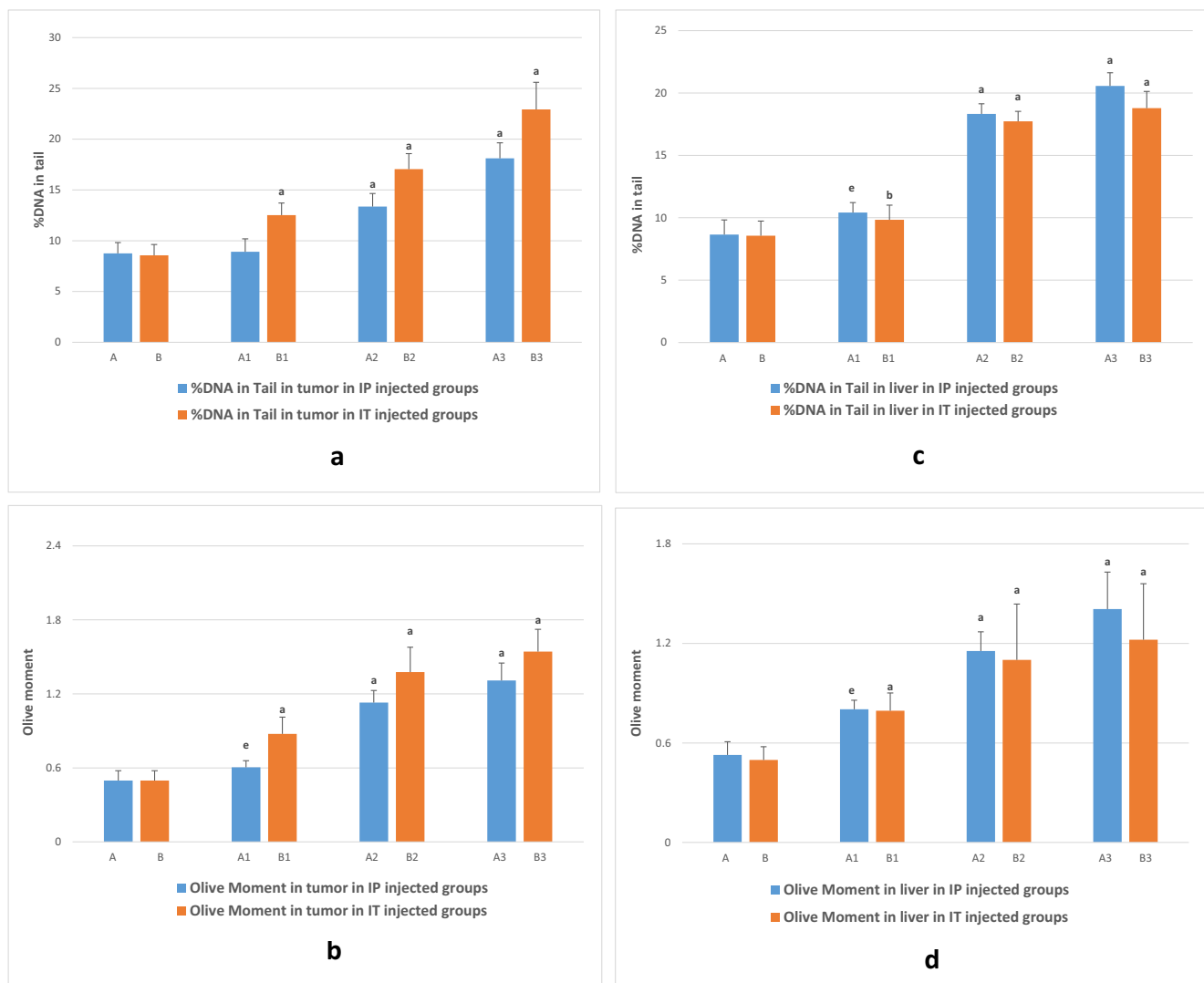


**Fig. 3** Modulation of comet parameters by different doses of AgNPs (6, 24, and 48 mg/kg) injected IP and IT observed in percent DNA in tail and olive moment: **a, b** in tumor and **c, d** in liver tissues. **e**: comet images of

tumor in all experimental groups. The data points are represented as mean  $\pm$  SD ( $n = 3$ ). (a,  $p \leq 0.0001$ ; b,  $p \leq 0.001$ ; c,  $p \leq 0.002$ ; d,  $p \leq 0.006$ ; e  $p \leq 0.01$ ) compared to the control group

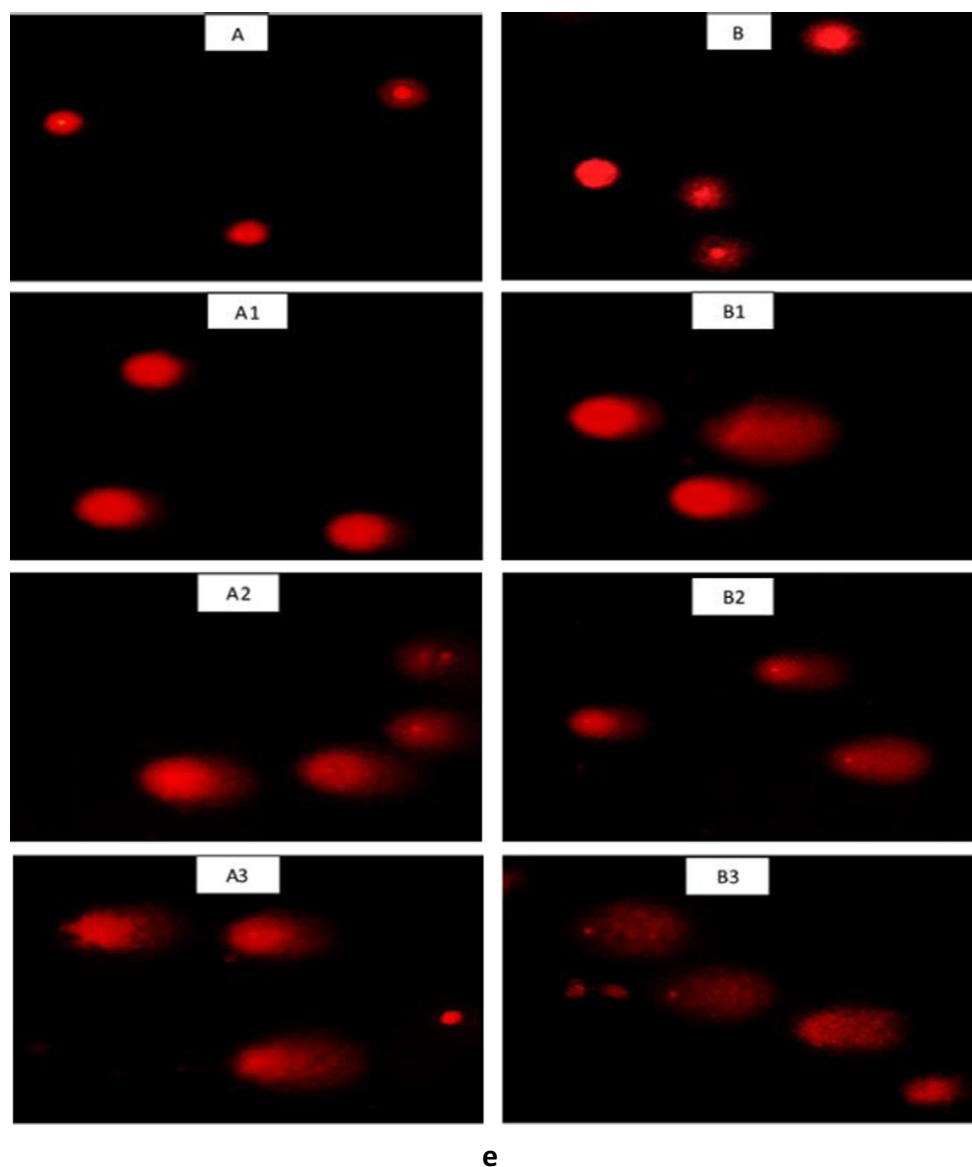


Fig. 3 (continued)

Figure 2c shows that treatment with AgNPs (administered either IP or IT) caused a noticeable decrease in SOD activity in tumor tissues in all groups by approximately 32 and 47% respectively compared to control groups. But these decrease was major in liver tissues when AgNPs were administered either IP or IT by approximately 46 and 64% respectively compared to control groups (Fig. 2d). Moreover, comparative analyses of these oxidative effects illustrated a relationship between the dose, method of AgNPs administered and the levels of MDA and the activity of SOD. These results are in accordance with many studies (Liu et al. 2015; El-Sonbaty 2013; Mansour et al. 2018; El Bialy et al. 2017), who reported that AgNPs are small with large surface areas; therefore, they have an ability to penetrate tissues and cells, generate ROS, inhibit antioxidant systems in blood and tissues of mice, and

be accompanied by an increase in lipid peroxide products. The level of MDA within cells can indicate the rate and intensity of lipid peroxidation within the body. Additionally, SOD activity directly reflects the antioxidant levels of the cell and body because it constitutes the first line of cellular defense against ROS.

ROS are highly reactive and result in oxidative damage, which is considered to be the major source of spontaneous damage to DNA (Cooke et al. 2003). Single cell gel electrophoresis from Ehrlich solid tumor and liver tissues showed comet formation in different treatment groups. Consequently, DNA damage was measured as percent tail DNA and olive tail moment in the control groups and in the treated animal groups (Fig. 3a–e). Mice groups treated with AgNPs (injected IP and IT)

exhibited significant increase percent DNA in tail in tumor cells by about 2- and 2.5-fold respectively compared to the control group (Fig. 3a). Also, Fig. 3c shows an increase in percent DNA in tail in liver cells in all groups treated with AgNPs and administered either IP or IT by approximately 3- and 2.5-fold respectively compared to the control group. These data were supported by the comet images in Fig. 3e and are in agreement with Jeyaraj et al. (2013). The explanation might be due to the small size and active surface of AgNPs, which allows it to penetrate the mitochondria and nuclear pore and also to create free radicals which induces a series of cytotoxic effects including generation of oxidative stress and leading to DNA damage (Zhang et al. 2014).

Liver tissue is responsible for detoxification once the organisms are treated with foreign substances. The present study revealed the histopathological changes in liver tissues caused by treatment with AgNPs (Fig. 4(I)). As shown in Fig. 4(I; B1), treatment with AgNPs (IT) at a dose of 6 mg/kg caused changes in the liver of mice as manifested by slight vacuolation of hepatocytes. These changes in the liver were increased in groups treated with high doses of 24 and 48 mg/kg (Fig. 4(I; B2, B3)) by congestion of hepatoportal blood vessel and portal infiltration with inflammatory cells, and hyperplasia of biliary epithelium and portal infiltration with inflammatory cells respectively compared to the control group (Fig. 4(I; B)). On the other hand, treatment with AgNPs (IP) amplified the changes in the liver of mice at a dose

of 6 mg/kg (Fig. 4(I; A1)), which was observed by cytoplasmic vacuolization of hepatocytes and congestion of hepatoportal blood vessel; occasional apoptosis and necrosis were observed in groups treated with high doses 24 and 48 mg/kg (Fig. 4(I; A2, A3)), by focal necrosis of hepatocytes associated with inflammatory cells infiltration and apoptosis of hepatocytes and sinusoidal leukocytosis respectively. Liver alteration in all treated groups was found dependent on the dose and way of AgNPs administrated. These observations are in accordance with the findings of previous studies (El Mahdy et al. 2014; Al Gurabi et al. 2015).

Treatment with AgNPs increased intracellular  $H_2O_2$  and induced DNA damage. These results are reflected by an increase in cell death as shown in the histopathological examination in the tissues of Ehrlich tumor (Fig. 4(II)). Masses of chromatophilic tumor cells between the necrotic muscles were observed in the control groups as shown in Fig. 4(II; A, B). Treatment with AgNPs (IT or IP) inhibits the promotion of Ehrlich carcinoma through masses of necrotic, fragmented tumor cells seen between the necrotic muscles in all treatments groups except the group treated with 6 mg/kg AgNPs (IP), which shows a mass of chromatophilic tumor cells between the necrotic muscles as the control group (Fig. 4(II; A1)).

The current results showed that oxidative stress, DNA damage, and histological changes induced by AgNPs result in some tumor shrinkages and the delay of tumor growth was obvious. Table 1 shows that the tumor volumes were suppressed in all groups treated with AgNPs

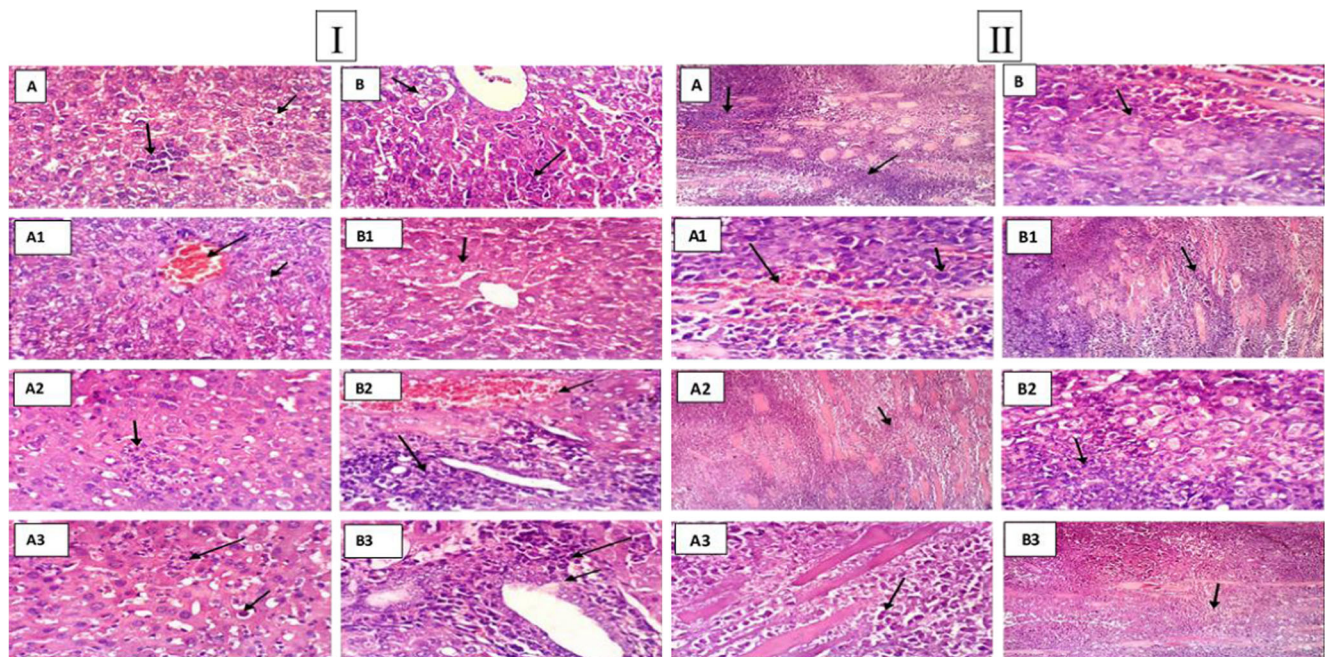


**Fig. 4** Liver (I) and tumor (II) histopathology photomicrographs in mice treated with different doses of AgNPs for (A1) and (B1): groups injected IP&IT by 6 mg/kg AgNPs, (A2) and (C2): groups injected IP&IT by

24 mg/kg AgNPs, (A3) and (B3): groups injected IP&IT by 48 mg/kg AgNPs and (A) and (B) control groups ( $\times 400$ )

**Table 1** Effect of AgNPs (6, 24, and 48 mg/kg) on tumor volume (cm<sup>3</sup>) in IP injected groups: (A1, A2, and A3), IT injected groups (B1, B2, and B3), and control groups (A and B)

		Days					
		Day 0	Day 3	Day 6	Day 9	Day 12	Day 15
Groups	A	0.30 ± 0.005	0.45 ± 0.0138	0.70 ± 0.02	0.88 ± 0.017	0.99 ± 0.1	1.14 ± 0.01
	A1	0.30 ± 0.019	0.41 ± 0.035	0.48 ± 0.02	0.57 ± 0.03	0.68 ± 0.02	0.78 ± 0.1
	A2	0.31 ± 0.0179	0.35 ± 0.014	0.33 ± 0.017	0.32 ± 0.02	0.29 ± 0.004	0.21 ± 0.02
	A3	0.31 ± 0.0178	0.30 ± 0.022	0.24 ± 0.005	0.19 ± 0.026	0.16 ± 0.01	0.12 ± 0.02
	B	0.30 ± 0.01	0.46 ± 0.014	0.71 ± 0.02	0.87 ± 0.02	1.02 ± 0.1	1.14 ± 0.01
	B1	0.30 ± 0.006	0.42 ± 0.012	0.57 ± 0.016	0.62 ± 0.025	0.64 ± 0.01	0.65 ± 0.003
	B2	0.30 ± 0.0184	0.43 ± 0.0139	0.36 ± 0.02	0.21 ± 0.012	0.14 ± 0.02	0.10 ± 0.01
	B3	0.30 ± 0.018	0.37 ± 0.0143	0.25 ± 0.013	0.13 ± 0.004	0.09 ± 0.003	0.05 ± 0.01

(A1, A2, A3, B1, B2, B3) at the end of treatment (day 15) by about 31, 81, 89, 42, 91, and 95% respectively compared to the control groups. These results confirm that AgNPs have the ability of producing free radical arising apoptosis and/or necrosis of tumor cells (El Bialy et al. 2017), as well as they approved that administration of AgNPs (IT) gave nearly good results than (IP). However, there is still more investigation needed to render the effective dose and the way of injection.

## Conclusion

AgNPs had the ability to induce various histopathological alterations in the tumor and liver indicating cytotoxicity probably by oxidative stress. Also, the induction of DNA damage in tumor and liver cells denoted the genotoxicity of AgNPs even with minor dose of 6 mg/kg. The cytotoxicity and genotoxicity of AgNPs depend on its concentration and the way of administration.

**Authors' contribution** M R and R G conceived and designed research, and analyzed data. MA conducted experiments and contributed new reagents or analytical tools. M R wrote the manuscript. All authors read and approved the manuscript.

## Compliance with ethical standards

**Conflict of interest** The authors declare that there are no conflicts of interest.

## References

Al Gurabi MA, Ali D, Alkahtani S, Alarifi S (2015) In vivo DNA damaging and apoptotic potential of silver nanoparticles in Swiss albino mice. *OncoTargets Ther* 8:295

- Avalos A, Haza AI, Mateo D, Morales P (2014) Cytotoxicity and ROS production of manufactured silver nanoparticles of different sizes in hepatoma and leukemia cells. *Appl Toxicol* 34:413–423
- Awara WM, El-Nabi SH, El-Gohary M (1998) Assessment of vinyl chloride-induced DNA damage in lymphocytes of plastic industry workers using a single-cell gel electrophoresis technique. *Toxicology* 128(1):9–16
- Awasthi KK, Awasthi A, Kumar N, Roy P, Awasthi K, John PJ (2013) Silver nanoparticle induced cytotoxicity, oxidative stress, and DNA damage in CHO cells. *J Nanopart Res* 15:1898
- Benn T, Cavanagh B, Hristovski K, Posner JD, Westerhoff P (2010) The release of nanosilver from consumer products used in the home. *J Environ Qual* 39(6):1875–1882
- Bergfeld SA, Blavier L, De Clerck YA (2014) Bone marrow-derived mesenchymal stromal cells promote survival and drug resistance in tumor cells. *Mol Cancer Ther* 13(4):962–975. <https://doi.org/10.1158/15357163.MCT-13-0400>
- Carlson C, Hussain SM, Schrand AM, Braydich-Stolle LK, Hess KL, Jones RL, Schlager JJ (2008) Unique cellular interaction of silver nanoparticles: size-dependent generation of reactive oxygen species. *J Phys Chem B* 112:13608–13619
- Chen X, Schluesener HJ (2008) Nanosilver: a nanoparticle in medical application. *Toxicol Lett* 176:1–12
- Cooke MS, Evans MD, Dizdaroglu M, Lunec J (2003) Oxidative DNA damage: mechanisms, mutation, and disease. *FASEB J* 17(10):1195–1214
- Ebabe Elle R, Gaillet S, Vidé J, Romain C, Lauret C, Rugani N, Cristol JP, Rouanet JM (2013) Dietary exposure to silver nanoparticles in Sprague-Dawley rats: effects on oxidative stress and inflammation. *Food Chem Toxicol* 60:297–301
- El Bialy BE, Hamouda RA, Khalifa KS, Hamza HA (2017) Cytotoxic effect of biosynthesized silver nanoparticles on Ehrlich ascites tumor cells in mice. *Int J Pharmacol*. <https://doi.org/10.3923/ijp.2017.134.144>
- El Mahdy MM, Salah Eldinb TA, Aly HS, Mohammed FF, Shaalan MI (2014) Evaluation of hepatotoxic and genotoxic potential of silver nanoparticles in albino rats. *Exp Toxicol Pathol* 67:21–29
- El-Bialy NS, Rageh MM (2013) Extremely low-frequency magnetic field enhances the therapeutic efficacy of low-dose cisplatin in the treatment of Ehrlich carcinoma. *BioMed Res Int* 2013:189352–189357
- El-Sonbaty SM (2013) Fungus-mediated synthesis of silver nanoparticles and evaluation of antitumor activity. *Cancer Nanotechnol* 4(4–5):73–79
- Foldbjerg R, Olesen P, Hougaard M, Dang DA, Hoffmann HJ, Autrup H (2009) PVP-coated silver nanoparticles and silver ions induce

- reactive oxygen species, apoptosis and necrosis in THP-1 monocytes. *Toxicol Lett* 190(2):156e62
- Gluga AR, Skoglund S, Wallinder IO, Fadeel B, Karlsson HL (2014) Size-dependent cytotoxicity of silver nanoparticles in human lung cells: the role of cellular uptake, agglomeration and ag release. *Part Fibre Toxicol* 11:11
- Gottesman MM, Fojo T, Bates SE (2002) Multi drug resistance in cancer: role of ATP-dependent transporters. *Nat Rev Cancer* 2(1):48–58
- Guo D, Zhu L, Huang Z, Zhou H, Ge Y, Mad W et al (2013) Anti-leukemia activity of PVP-coated silver nanoparticles via generation of reactive oxygen species and release of silver ions. *Biomaterials* 34(32):7884–7894
- Gurunathan S, Han JW, Eppakayala V, Jeyaraj M, Kim JH (2013a) Cytotoxicity of biologically synthesized silver nanoparticles in MDA-MB-231 human breast cancer cells. *Biomed Res Int* 2013:535796
- Gurunathan S, Raman J, Abd Malek SN, John PA, Vikineswary S (2013b) Green synthesis of silver nanoparticles using *Ganoderma neo-japonicum* Imazeki: a potential cytotoxic agent against breast cancer cells. *Int. J Nanomedicine* 8:4399–4413
- Han JW, Gurunathan S, Jeong JK, Choi YJ, Kwon DN, Park JK, Kim JH (2014) Oxidative stress mediated cytotoxicity of biologically synthesized silver nanoparticles in human lung epithelial adenocarcinoma cell line. *Nanoscale Res Lett* 9(1):459
- Hill GW, Morest DK, Parham K (2008) Cisplatin-induced ototoxicity: effect of in tatympnic dexamethasone injections. *Otol. Neurotol* 29:1005–1011
- Jeyaraj M, Sathishkumar G, Sivanandhan G, MubarakAli D, Rajesh M, Arun R, Kapildev G, Manickavasagam M, Thajuddin N, Premkumar K, Ganapathi A (2013) Biogenic silver nanoparticles for cancer treatment: an experimental report. *Colloids Surf B: Biointerfaces* 106:86–92
- Kalishwaralal K, Banumathi E, Pandian SBRK, Deepak V, Muniyandi J, Eom SH, Gurunathan S (2009) Silver nanoparticles inhibit VEGF induced cell proliferation and migration in bovine retinal endothelial cells. *Colloids Surf B Biointerfaces* 73:51–57
- Kim S, Ryu DY (2013) Silver nanoparticle-induced oxidative stress, genotoxicity and apoptosis in cultured cells and animal tissues. *J Appl Toxicol* 33:78–89
- Kim JS, Kuk E, Yu KN, Kim JH, Park SJ, Lee HJ, Kim SH, Park YK, Park YH, Hwang C, Kim Y, Lee Y, Jeong DH, Cho M (2007) Antimicrobial effects of silver nanoparticles, *Nanomed. Nanotechnol Biol Med* 3:95–101
- Kim KJ, Sung WS, Suh BK, Moon SK, Choi JS, Kim JG, Lee DG (2009) Antifungal activity and mode of action of silver nanoparticles on *Candida albicans*. *Biometals* 22:235–242
- Kwon JT, Tehrani AM, Hwang SK, Kim JE, Shin JY, Yu KN, Chang SH, Kim DS, Kwon YT, Choi IJ, Cheong YH, Kim JS, Cho MH (2012) Acute pulmonary toxicity and body distribution of inhaled metallic silver nanoparticles. *Toxicol Res* 28(1):25–31
- Lin CX, Yang SY, Gu JL, Meng J, Xu HY, Cao JM (2017) The acute toxic effects of silver nanoparticles on myocardial transmembrane potential,  $I_{Na}$  and  $I_{K1}$  channels and heart rhythm in mice. *Nanotoxicology* 11(6):827–837. <https://doi.org/10.1080/17435390.2017.1367047>
- Liu HL, Yang HL, Lin BC, Zhang W, Tian L, Zhang HS, Xi ZG (2015) Toxic effect comparison of three typical sterilization nanoparticles on oxidative stress and immune inflammation response in rats. *Toxicol Res* 4(2):486–493
- Mansour HH, Eid M, El-Amaouty MB (2018) Effect of silver nanoparticles synthesized by gamma radiation on the cytotoxicity of doxorubicin in human cancer cell lines and experimental animals. *Human Exp Toxicol* 37(1):38–50
- Mata R, Nakkala JR, Chandra VK, Raja K, Sadras SR (2018) In vivo bio-distribution, clearance and toxicity assessment of biogenic silver and gold nanoparticles synthesized from *Abutilon indicum* in Wistar rats. *J Trace Elem Med Biol* 48:157–165. <https://doi.org/10.1016/j.jtemb.2018.03.015>
- Moller P (2006) The alkaline comet assay: towards validation in biomonitoring of DNA damaging exposures. *Basic Clin Pharmacol Toxicol* 98:336–345
- Moller P, Knudsen LE, Loft S, Wallin H (2000) The comet assay as a rapid test in biomonitoring occupational exposure to DNA damaging agents and effect of confounding factors. *Cancer Epidemiol Biomark Prev* 9(10):1005–1015
- Narchin F, Larijani K, Rustayan A, Nejad Ebrahimi S, Tafvizi F (2018) Phytochemical synthesis of silver nanoparticles by two techniques Using *Saturaja* rechengri Jamzad extract: identifying and comparing *in Vitro* anti-proliferative activities. *Adv Pharm Bull* 8:235–244
- Ning S, Macleod K, Abra RM, Huang AH, Hahn GM (1994) Hyperthermia induces doxorubicin release from long-circulating liposomes and enhances their anti-tumor efficacy. *Int J Radiat Oncol Biol Phys* 29(4):827–834
- Nishikimi M, Appaji Rao N, Yagi K (1972) The occurrence of superoxide anion in the reaction of reduced phenazine methosulfate and molecular oxygen. *Biochem Biophys Res Commun* 46:849–854
- Pacioni NL, Borsarelli CD, Rey V, Veglia AV. Synthetic routes for the preparation of silver nanoparticles. In *Silver Nanoparticle Applications* 2015 (pp. 13–46). Springer, Cham.
- Park S, Lee YK, Jung M, Kim KH, Chung N, Ahn EK, Lim Y, Lee KH (2007) Cellular toxicity of various inhalable metal nanoparticles on human alveolar epithelial cells. *Inhal Toxicol* 19(Suppl 1):59–65
- Park MV, Neigh AM, Vermeulen JP, de la Fonteyne LJ, Verharen HW, Briede JJ, Van LH, De Jong WH (2011) The effect of particle size on the cytotoxicity, inflammation, developmental toxicity and genotoxicity of silver nanoparticles. *Biomaterials* 32:9810–9817
- Piao MJ, Kang KA, Lee IK, Kim HS, Kim S, Choi JY et al (2011) Silver nanoparticles induce oxidative cell damage in human liver cells through inhibition of reduced glutathione and induction of mitochondria-involved apoptosis. *Toxicol Lett* 201(1):92e100
- Prasannaraj G, Sahi SV, Ravikumar S, Venkatachalam P (2016) Enhanced cytotoxicity of biomolecules loaded metallic silver nanoparticles against human liver (HepG2) and prostate (PC3) cancer cell lines. *J Nanosci Nanotechnol* 16(5):4948–4959
- Rageh M. M., El-Gebaly R. H., (2018) Melanin nanoparticles: antioxidant activities and effects on  $\gamma$ -ray-induced DNA damage in the mouse. *Mutat Res Gen Tox En* 15–22
- Ratyakshi CRP (2009 Jan 1) Colloidal synthesis of silver nanoparticles. *Asian J Chem* 21(10):S113–S116
- Scoville DK, Botta D, Galdanes K, Schmuck SC, White CC, Stapleton PL, Bammler TK, MacDonald JW, Altemeier WA, Hernandez M, Kleeberger SR, Chen LC, Gordon T, Kavanagh TJ (2017) Genetic determinants of susceptibility to silver nanoparticle-induced acute lung inflammation in mice. *FASEB J* 31(10):4600–4611. <https://doi.org/10.1096/fj.201700187R>
- Siegel RL, Miller KD, Jemal A (2016) Cancer statistics, 2016. *CA Cancer J Clin* 66(1):7–30. <https://doi.org/10.3322/caac.21332>
- Singh NP, McCoy MT, Tice RR, Schneider EL (1988) A simple technique for quantitation of low levels of DNA damage in individual cells. *Exp Cell Res* 175(1):184–191
- Swain SM, Whaley FS, Ewer MS (2003) Congestive heart failure in patients treated with doxorubicin: a retrospective analysis of three trials. *Cancer* 97:2869–2879
- Swanner J, Mims J, Carroll DL, Akman SA, Furdul CM, Torti SV, Singh RN (2015) Differential cytotoxic and radiosensitizing effects of silver nanoparticles on triple-negative breast cancer and non-triple-negative breast cells. *Int J Nanomedicine* (10):3937–3953
- Thakkar KN, Mhatre SS, Parikh RY (2010) Biological synthesis of metallic nanoparticles. *Nanomed NBM* 6(2):257–262
- Tice RR, Agurell E, Anderson D, Burlinson B, Hartmann A, Kobayashi H, Miyamae Y, Rojas E, Ryu JC, Sasaki YF (2000) Single cell gel/comet assay: guidelines for in vitro and in vivo genetic toxicology testing. *Environ Mol Mutagenesis* 35(3):206–221

- Tiwari DK, Jin T, Behari J (2011) Dose-dependent in-vivo toxicity assessment of silver nanoparticle in Wistar rats. *Toxicol Mech Methods* 21(1):13–24
- Turkevich J, Stevenson PC, Hillier J (1951) A study of the nucleation and growth processes in the synthesis of colloidal gold. *Discuss Faraday Soc* 11:55–75
- Uchiyama M, Mihara M (1978) Determination of malonaldehyde precursor in tissues by thiobarbituric acid test. *Anal Biochem* 86:271–278
- Wen H., Dan M., Yang Y., Lyu J., Shao A., Cheng X., Chen L., Xu L., (2017) Acute toxicity and genotoxicity of silver nanoparticle in rats. *PLOS ONE*
- Yuan YG, Peng QL, Gurunathan S (2017) Silver nanoparticles enhance the apoptotic potential of gemcitabine in human ovarian cancer cells: combination therapy for effective cancer treatment. *Int J Nanomedicine* 12:6487–6502. <https://doi.org/10.2147/IJN.S135482>
- Zapór L (2016) Effects of silver nanoparticles of different sizes on cytotoxicity and oxygen metabolism disorders in both reproductive and respiratory system cells. *Arch Environ Prot* 42(4):32–47
- Zhang T, Wang L, Chen Q, Chen C (2014) Cytotoxic potential of silver nanoparticles. *Yonsei Med J* 55(2):283–291
- Zhou G, Wang W (2012) Synthesis of silver nanoparticles and their antiproliferation against human lung cancer cells in vitro. *Orient J Chem* 28(2):651–655
- Zielinska E, Zauszkiewicz-Pawlak A, Wojcik M, Inkielewicz-Stepniak I (2018) Silver nanoparticles of different sizes induce a mixed type of programmed cell death in human pancreatic ductal adenocarcinoma. *Oncotarget* 9(4):4675–4697